Summary. This paper deals with an issue of Mathematical Physics and Computation. More precisely, the distribution of eigenvalues per unit volume is estimated for Hamiltonians occurring in quantum models of disordered solids. While rigorous analytical results had been known for regular single-site distributions the problem was open for singular ones, especially for the Bernoulli–Anderson model.

Here we present some numerical and analytical results concerning the occurrence of peaks in the density of states. To rule out such peaks is the major stumbling block on the way to prove (analytically) that localization occurs at low energies.

The computational challenge in this project comes from the following fact: Very high precision is needed and large matrices have to be diagonalized to enter the regime where selfaveraging overrules those peaks in the eigenvalue distribution that simply come from finite-size effects. Large samples have to be investigated to obtain results of statistical relevance.

The analytical challenge comes from the fact that all previously known methods relied on the continuity of the single-site distribution defining the model and fail completely for the most prominent example with a singular distribution: the Bernoulli–Anderson model.

Fine structure of the integrated density of states for Bernoulli–Anderson models

P. Karmann[1], R. A. Römer[2], M. Schreiber[1], and P. Stollmann[3]

[1] Institut für Physik, Technische Universität Chemnitz, 09107 Chemnitz, Germany
[2] Department of Physics and Centre for Scientific Computing, University of Warwick, Coventry, CV4 7AL, United Kingdom
[3] Fakultät für Mathematik, Technische Universität Chemnitz, 09107 Chemnitz, Germany

1 Introduction

Disorder is one of the fundamental topics in science today. A very prominent example is Anderson's model [1] for the transition from metal to insulator under the presence of disorder.

Apart from its intrinsic physical value this model has triggered an enormous amount of research in the fields of random operators and numerical analysis, resp. numerical physics. As we will explain below, the Anderson model poses extremely hard problems in these fields and so mathematical rigorous proofs of many well substantiated findings of theoretical physics are still missing. The very nature of the problem also causes highly nontrivial challenges for numerical studies.

The transition mentioned above can be reformulated in mathematical terms in the following way: for a certain random Hamiltonian one has to prove that its spectral properties change drastically as the energy varies. For low energies the spectrum is pure point, with eigenfunctions that decay exponentially. This energy regime is called localization.

For energies away from the spectral edges, the spectrum is expected to be absolutely continuous, providing for extended states that can lead to transport. Sadly enough, more or less nothing has been proven concerning the second kind of spectral regime, called delocalization. An exception are results on trees [2, 3], and for magnetic models [4]. Anyway, there are convincing theoretical arguments and numerical results that support the picture of the metal–insulator transition (which is, in fact, a dimension-dependent effect and should take place for dimensions $d > 2$).

In our research we are dealing with a different circle of questions. The Anderson model is in fact a whole class of models: an important input is the measure μ that underlies the random onsite couplings. In all proofs of localiza-

tion (valid for $d > 1$) one needs regularity of this measure μ. This excludes a prominent and attractive model: the Anderson model of a binary alloy, i.e. two kinds of atoms randomly placed on the sites of a (hyper)cubic lattice, known as Bernoulli–Anderson model in the mathematical community. Basically there are two methods of proof for localization: multiscale analysis [5], and the fractional moment method [6]. In both cases one needs an a-priori bound on the probability that eigenvalues of certain Hamiltonians cluster around a fixed energy, i.e., one has to exclude resonances of finite box Hamiltonians. Equivalently, one needs a weak kind of continuity of the integrated density of states. In multiscale analysis this a-priori estimate comes in a form that is known as Wegner's estimate [7]. Here we will present both rigorous analytical results and numerical studies of these resonances. We will take some time and effort to describe the underlying concepts and ideas in the next Section. Then we remark recent progress concerning analytical results. Here one has to mention a major breakthrough obtained in a recent paper [8] of J. Bourgain and C. Kenig who prove localization for the continuum Bernoulli–Anderson model in dimensions $d \geq 2$. Finally, we display our numerical studies and comment on future directions of research.

We conclude this section with an overview over recent contributions in the physics literature concerning the binary-alloy model. These may be classified into mainly simulations or mainly theoretical analyses. The former are discussed in [9], albeit in the restricted setting of a Bethe lattice, providing a detailed analysis of the electronic structure of the binary-alloy and the quantum-percolation model, which can be derived from the binary alloy replacing one of the alloy constituents by vacancies. The study is based on a selfconsistent scheme for the distribution of local Green functions. Detailed results for the local density of states (DOS) are obtained, from which the phase diagram of the binary alloy is constructed. The existence of a quantum-percolation threshold is discussed. Another study [10] of the quantum site-percolation model on simple cubic lattices focuses on the statistics of the local DOS and the spatial structure of the single particle wave functions. By using the kernel polynomial previous studies of the metal–insulator transition are refined and the nonmonotonic energy dependence of the quantum-percolation threshold is demonstrated. A study of the three-dimensional binary-alloy model with additional disorder for the energy levels of the alloy constituents is presented in [11]. The results are compared with experimental results for amorphous metallic alloys. By means of the transfer-matrix method, the metal–insulator transitions are identified and characterized as functions of Fermi-level position, band broadening due to disorder and alloy composition. The latter is also investigated in [12], which discusses the conditions to be put on mean-field-like theories to be able to describe fundamental physical phenomena in disordered electron systems. In particular, options for a consistent mean-field theory of electron localization and for a reliable description of transport properties are investigated. In [13] the single-site coherent potential approximation is extended to include the effects of non-local disorder correlations (i.e. alloy

short-range order) on the electronic structure of random alloy systems. This is achieved by mapping the original Anderson disorder problem to that of a selfconsistently embedded cluster. The DOS of the binary-alloy model has been studied in [14], where also the mobility edge, i.e. the phase boundary between metallic and insulating behaviour was investigated. The critical behaviour, in particular the critical exponent with which the localization length of the electronic states diverges at the phase transition was analyzed in [15] in comparison with the standard Anderson model.

2 Resonances and the integrated density of states

2.1 Wegner estimates, IDS, and localization

In this Section we sketch the basic problem and introduce the model we want to consider. A major point of the rather expository style is to make clear, why the problem is as difficult as it appears to be. This also sheds some light on why it is intrinsically hard to study numerically. Let us first write down the Hamiltonian in an analyst's notation:

On the Hilbert space $\ell^2(\mathbb{Z}^d)$ we consider the random operator

$$H(\omega) = -\Delta + V_\omega,$$

where the discrete Laplacian incorporates the constant (nonrandom) off-diagonal or hopping terms. It is defined, for $\psi \in \ell^2(\mathbb{Z}^d)$ by

$$\Delta\psi(i) = \sum_{|i-j|=1} \psi(j)$$

for $i \in \mathbb{Z}^d$. This reflects that we are dealing with a nearest neighbor interaction, where the value of the wave function at site i is only influenced by those at the $2d$ neighbors on the integer lattice. The random potential V_ω is, in its simplest form, given by independent identically distributed (short: i.i.d.) random variables at the different sites. A convenient representation is given in the following way:

$$\Omega = \Pi_{i\in\mathbb{Z}^d}\mathbb{R}, \mathbb{P} = \Pi_{i\in\mathbb{Z}^d}\mu, V_\omega(i) = \omega_i$$

where μ is a probability measure on the real line. This gives the random diagonal multiplication operator acting as

$$V_\omega\psi(i) = \omega_i\psi(i).$$

For simplicity we assume that the support of the so-called single-site measure μ is a compact set $K \subset \mathbb{R}$. Put differently, for every site i we perform a random experiment that gives the value ω_i distributed according to μ. In physicist's notation we get

$$H(\omega) = \sum_{\langle i,j \rangle} |i\rangle\langle j| + \sum_i \omega_i |i\rangle\langle i|,$$

where $|i\rangle$ denotes the basis functions in site representation.

In principle, one expects that the spectral properties should not depend too much on the specific distribution μ (apart from the very special case that μ reduces to a point mass, in which case there is no disorder present). Let us take a look at two very different cases. In the Bernoulli–Anderson model we have the single-site measure $\mu = \frac{1}{2}\delta_0 + \frac{1}{2}\delta_1$. In that case the value $\omega_i \in \{0, 1\}$ is determined by a fair coin. We will also consider a coupling parameter W in the random part, in which case we have either $\omega_i = 0$ or $\omega_i = W$ each with probability $\frac{1}{2}$. The resulting random potential is denoted by V_ω^B. In the second case the potential value is determined with respect to the uniform distribution so that we get $\mu(dx) = \chi_{[0,1]}(x)dx$. We write V_ω^U for this case.

Let us point out one source of the complexity of the problem: The two operators that sum up to $H(\omega)$ are of very different nature:

- The discrete Laplacian is a difference operator. It is diagonal in Fourier space $L^2(\mathbb{T}^d)$, where it is given by multiplication with the function

$$\sum_{k=1}^{d} 2\cos x_k.$$

  Therefore, its spectrum is given by the range of this function, so that

$$\sigma(-\Delta) = [-2d, 2d],$$

  the spectrum being purely absolutely continuous.
- The random multiplication operator V_ω is diagonal in the basis $\{\delta_i | i \in \mathbb{Z}^d\}$. The spectrum is hence the closure of the range of V_ω, which is just the support K of the measure for $\mathbb{P}$–a.e.$\omega \in \Omega$ (a.e. stands for almost every, i.e., for all but a set of measure zero). In the aforementioned special cases we get

$$\sigma(V_\omega^B) = \{0, 1\}$$

  for the Bernoulli–Anderson model and

$$\sigma(V_\omega^U) = [0, 1],$$

  both for a.e. $\omega \in \Omega$. Clearly, the spectral type is pure point with perfectly localized eigenfunctions for every ω, the set of eigenvalues being given by $\{\omega_i | i \in \mathbb{Z}^d\}$.

One major problem of the analysis as well as the numerics is now obvious: We add two operators of the same size with completely different spectral type and there is no natural basis to diagonalize the sum $H(\omega) = -\Delta + V_\omega$, since one of the two terms is diagonal in position space while the other is diagonal in momentum space (the Fourier picture).

Another cause of difficulties is the expected spectral type of $H(\omega)$. In the localized regime it has a dense set of eigenvalues. These eigenvalues are extremely unstable. Rank-one perturbation theory gives the following fact which illustrates this instability: If we fix all values ω_j except one, say ω_i and vary the latter continuously in an interval, the resulting spectral measures will be mutually singular and for a dense set of values of ω_i the spectrum will contain a singular continuous component, cf. [16].

Moreover, the qualitative difference between the Bernoulli–Anderson model and the model with uniform distribution is evident: V_ω^U displays the spectral type we want to prove for $H(\omega)$: it has a dense set of eigenvalues for a.e. ω. If one can treat $-\Delta$ in some sense as a small perturbation we arrive at the desired conclusion. In view of the preceding paragraph, this cannot be achieved by standard perturbation arguments. In the Bernoulli–Anderson model V_ω^B has only eigenvalues 0 and 1, each infinitely degenerate.

In typical proofs of localization an important tool is the study of box Hamiltonians. To explain this, we consider the cube $\Lambda_L(i)$ of side length L centered at i. We restrict $H(\omega)$ to the sites in $\Lambda_L(i)$ which constitutes a subspace of dimension $|\Lambda_L(i)| = L^d$. We denote the restriction by $H_L(\omega)$ and suppress the boundary condition, since it does not play a role in asymptotic properties as $L \to \infty$.

These box Hamiltonians enter in resolvent expansions and it is important to estimate the probability that their resolvents have a large norm, i.e., we are dealing here with small-denominator problems. Since the resolvent has large norm for energies near the spectrum one needs upper bounds for

$$\mathbb{P}\{\sigma(H_L(\omega)) \cap [E-\epsilon, E+\epsilon] \neq \emptyset\} = p(\epsilon, L).$$

In fact, one wants to show that $p(\epsilon, L)$ is small for large L and small ϵ. At the same time, there is a clear limitation to such estimates: In the limit $L \to \infty$ the spectra of $H_L(\omega)$ converge to the spectrum of $H(\omega)$. This means that for fixed $\epsilon > 0$ and $E \in \sigma(H(\omega))$ (and only those energies E are of interest),

$$p(\epsilon, L) \to 1 \text{ for } L \to \infty.$$

The famous Wegner estimate [7] states that for absolutely continuous μ we get

$$p(\epsilon, L) \leq C\epsilon L^d, \tag{1}$$

where the last factor is the volume of the cube $|\Lambda_L(i)| = L^d$. This estimate is sufficient for a proof of localization for energies near the spectral edges. The proof is not too complicated for the discrete model. To see why it might be true, let us include a very simple argument in the case that there is no hopping term.

Then

$$\begin{aligned}\mathbb{P}\{\sigma(V_\omega) \cap [E-\epsilon, E+\epsilon] \neq \emptyset\} &= \mathbb{P}\{\exists j \in \Lambda_L \text{ s.t. } V_\omega(j) \in [E-\epsilon, E+\epsilon]\} \\ &\leq |\Lambda_L| \cdot \mu[E-\epsilon, E+\epsilon] \\ &\leq C \cdot |\Lambda_L| \cdot \epsilon,\end{aligned}$$

if μ is absolutely continuous. Here we see that the situation is completely different for the Bernoulli–Anderson model for which $\mu[E-\epsilon, E+\epsilon] \geq \frac{1}{2}$ whenever $E \in \{0, 1\}$. Also, it is clear that a Wegner estimate of the type (1) above cannot hold. Since in

$$\mathbb{P}\{\sigma(H_L(\omega)) \cap [E-\epsilon, E+\epsilon] \neq \emptyset\}$$

only $2^{|\Lambda_L|}$ Bernoulli variables are comprised, this probability must at least be $2^{-|\Lambda_L|}$, unless it vanishes.

The Wegner estimate is intimately related to continuity properties of the integrated density of states (IDS), a function $N : \mathbb{R} \to [0, \infty)$ that measures the number of energy levels per unit volume:

$$N(E) = \lim_{L\to\infty} \frac{1}{|\Lambda_L|} \mathbb{E}(\mathrm{Tr}\chi_{(-\infty,E]}(H_L(\omega))).$$

Here $\chi_{(-\infty,E]}(H_L(\omega))$ is the projection onto the eigenspace spanned by the eigenvectors with eigenvalue below E and the trace determines the dimension of this space, i.e., the number of eigenvalues below E counted with their multiplicity. Since we are dealing with operators of rank at most $|\Lambda_L|$, we get

$$\begin{aligned} N(E+\epsilon) - N(E-\epsilon) &\approx \frac{1}{|\Lambda_L|} \mathbb{E}(\mathrm{Tr}\chi_{(E-\epsilon,E+\epsilon]}(H_L(\omega))) \\ &\leq \mathbb{P}\{\sigma(H_L(\omega)) \cap [E-\epsilon, E+\epsilon] \neq \emptyset\}. \end{aligned}$$

This means that Wegner estimates lead to continuity of the IDS. Although that is not clear from the above rather crude reasoning, the Wegner estimate for absolutely continuous μ yields differentiability of the IDS.

2.2 Recent rigorous analytical results

In this section we will mainly be dealing with continuum models,

$$H(\omega) = -\Delta + V_\omega,$$

where $-\Delta$ is now the unbounded Laplacian with domain $W^{2,2}(\mathbb{R}^d)$, the Sobolev space of square integrable functions with square integrable second partial derivatives. The random multiplication operator V_ω is defined by

$$V_\omega(x) = \sum_{i\in\mathbb{Z}^d} \omega_i u(x-i),$$

with a single-site potential $u \geq 0$ bounded and of compact support (for simplicity reasons), and random coupling like above. Some results we mention are valid under more general assumptions, as can be seen in the original papers. For results concerning localization of these models we refer to [5] for a survey of the literature up to 2000. More recent results concerning the IDS and its continuity properties can be found in [17]. Here we will report on more recent developments. The first result is partly due to one of us [18].

Theorem 1. *Let $H(\omega)$ be an alloy-type model and $u \geq \kappa\chi_{[-1/2,1/2]^d}$ for some positive κ. Then for each $E_0 \in \mathbb{R}$ there exists a constant C_W such that, for all $E \leq E_0$ and $\varepsilon \leq 1/2$*

$$\mathbb{E}\{\mathrm{Tr}[\chi_{[E-\varepsilon,E+\varepsilon]}(H_L(\omega))]\} \leq C_W \; s(\mu,\varepsilon)\,(\log \tfrac{1}{\varepsilon})^d \; |\Lambda_L|, \tag{2}$$

where

$$s(\mu,\varepsilon) = \sup\{\mu([E-\varepsilon, E+\varepsilon]) \mid E \in \mathbb{R}\}. \tag{3}$$

The mentioned alloy-type models include the models we introduced as well as additional periodic exterior potentials and magnetic vector potentials. The idea of the proof is to combine methods from [19] with a technique to control the influence of the kinetic term: the estimate in [19] is quadratic in the volume of the cube and so it cannot be used to derive continuity of the IDS. On the other hand, there had been recent progress for models with absolutely continuous μ [20, 21, 22] using the spectral shift function. In [18] we present an improved estimate of the spectral shift function and apply it to arrive at the estimate (2). Of course, the latter is not really helpful, unless the measure μ shares a certain continuity. Still it is interesting in so far that it yields that N is nearly as continuous as μ with a logarithmically small correction. For more details we refer to [18], where the reader can also find a detailed account of how our result compares with recent results in this direction.

We now mention a major breakthrough obtained in the recent work [8] where the continuum Bernoulli–Anderson model is treated. For this model, the authors set up a multi-scale induction to prove a Wegner estimate of the following type:

Theorem 2. *For the Bernoulli–Anderson model and $\alpha, \beta > 0$ there exist $C, \gamma > 0$ such that*

$$\mathbb{P}\{\sigma(H_L(\omega)) \cap [E-\epsilon, E+\epsilon] \neq \emptyset\} \leq C L^{-\frac{1}{2}d+\alpha}$$

for

$$\epsilon \leq \exp(-\gamma L^{\frac{4}{3}+\beta}).$$

This can be found as Lemma 5.1 in [8]. It is important to note that the proof does not so far extend to the discrete case. The reason is that a major step in the proof is a quantitative unique continuation result that does not extend to the discrete setting. Therefore, Wegner estimates for the discrete Bernoulli–Anderson model are still missing.

3 Numerical studies

Most numerical studies have been performed for the standard Anderson model of localization with uniform distribution of the potential values. In this model the DOS changes smoothly with increasing disorder from the DOS of the

Laplacian with its characteristic van Hove singularities to one featureless band [23]. If the distribution is chosen as common with mean 0 and width W, then the theoretical band edges are given by $\pm(2d + W/2)$. Numerically these values are of course reached with vanishing probability. If the box distribution is replaced by an unbounded distribution like the Gaussian or the Lorentzian, then the band tails in principle extend to infinity, although numerically no significant change can be observed from the box-distribution case [24]. A dramatically different situation occurs in a binary alloy, where with increasing disorder W the DOS separates into two bands of width $4d$ each. Choosing the measure $\mu = \frac{1}{2}\delta_0 + \frac{1}{2}\delta_W$ as discussed in the previous section, the splitting of the band into subbands occurs theoretically for $W = 4d$, although the again numerically very small DOS in the tails of the subbands leads to the appearance of separated subbands for smaller disorder values already [14]. This, however, is not the topic of the current investigation. We rather concentrate on unexpected structures that we have found near the centre of the subbands.

The DOS is defined as usual

$$\rho(E) = \left\langle \sum_{i=1}^{L^d} \delta(E - E_i) \right\rangle$$

where E_i are the eigenvalues of the box Hamiltonian discussed in the previous section, and $\langle \cdots \rangle$ indicates the average over an ensemble of different configurations of the random potential, i.e. the disorder average. For the numerical diagonalization we use the Lanczos algorithm [25] which is very effective for sparse matrices. In the present case the matrices are extremely sparse, because except for the diagonal matrix element with the potential energy there are only 6 elements in each row and column of the secular matrix due to the Laplacian. In fact, for the standard model of Anderson localization which is of course as sparse as the Bernoulli–Anderson Hamiltonian matrix the Lanczos algorithm has been shown to be most effective also in comparison with more modern eigenvalue algorithms [26, 27]. One of the reasons for the difficulties which all eigenvalue algorithms encounter is our use of periodic boundary conditions in all directions, making a transformation of the secular matrix to a band matrix impossible. However, a severe problem arises for the Lanczos algorithm, because numerical inaccuracies due to finite precision arithmetics yield spurious eigenvalues which show up as incorrectly multiple eigenenergies. In principle these can be detected and eliminated in a straightforward way. The respective procedure, however, becomes ineffective in those parts of the spectrum where the Hamiltonian itself has multiple eigenvalues or an unusually large DOS. This happens to be the case in our investigation and turned out to be more significant for larger disorder and system sizes. As a consequence we have missed up to .09 % of all eigenvalues in the data presented below. In general, the performance of the Lanczos algorithm is much better in the band tails, because the convergence is much faster. Therefore it turned out to be advantageous to calculate the DOS in the centre of the

subbands separately with different settings of the parameters which control the convergence of the algorithm.

Our results are shown in Fig. 1 for various disorders. Here we have chosen a symmetric binary distribution, i.e. $\mu = \frac{1}{2}\delta_{-W/2} + \frac{1}{2}\delta_{W/2}$. The spectrum is thus symmetric with respect to $E = 0$ and only the upper subband is displayed in Fig. 1. With increasing disorder strength W, the subband moves of course to larger energies. Already for $W = 8$ the subbands appear to be separated, as the DOS is numerically zero around $E = 0$. We have also calculated the DOS for the system size $L = 15$ for disorders between $W = 4$ and $W = 22.6$. The data are not shown in Fig. 1, because they do not significantly differ from the data for the larger system size $L = 30$ shown in the plot. Only for $W = 2$ there are significant deviations due to finite-size effects: for vanishing disorder the finite size of the system with its periodic boundaries would yield only very few but highly multiple eigenvalues. Remnants of such structures can be seen in the inset of Fig. 1 for the smaller system size as somewhat smeared-out peaks. For the larger system size $L = 30$ the DOS in the inset reflects the DOS of the pure Laplacian with only a weak smearing of the van Hove singularities.

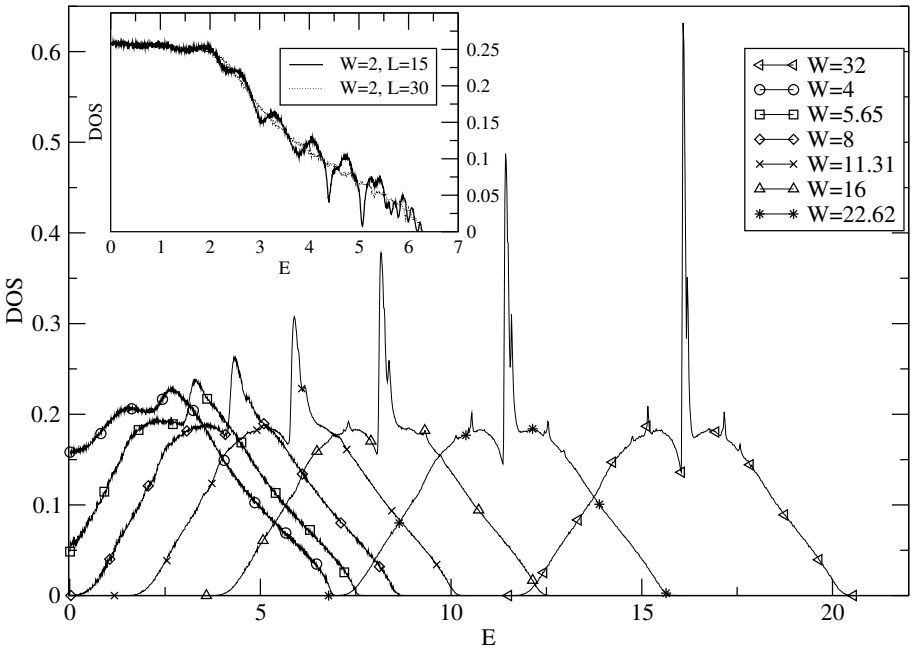

Fig. 1. DOS of the upper half of the spectrum for several disorder strengths W and system sizes $L = 30$ averaged over 250 configurations of disorder except for $W = 32$, where the system size is $L = 15$ and 2000 configurations have been used. The inset shows the DOS for $W = 2$, $L = 15$ and 30.

The prominent feature of the spectra is a strong peak in the centre of the subband accompanied by a distinguished minimum on the low energy site and a side peak on the right hand shoulder. In order to study the emergence of these features we have plotted the central region of the subbands in Fig. 2 versus scaled energy thus eliminating the shift of subbands with increasing disorder. One can clearly see, that the peak and the minimum close to it approach the centre of the subband.

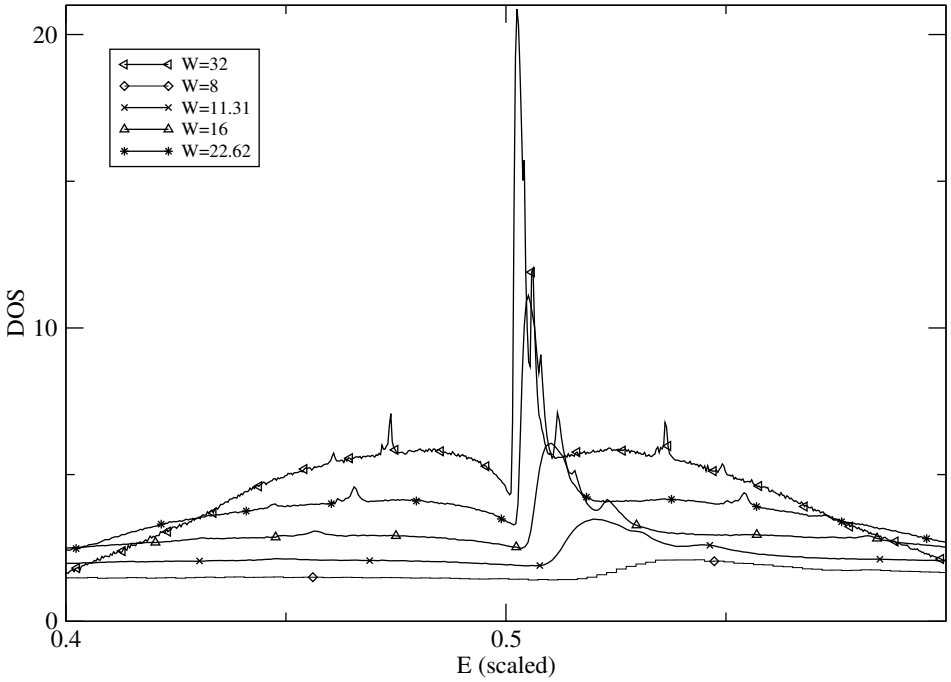

Fig. 2. DOS of the upper subband from Fig. 1 with all eigenvalues scaled by W. The DOS has been normalized after rescaling.

The maximum and minimum values of the DOS can be described by power laws

$$\rho_{\max} \propto W^{\beta}, \quad \beta = 1.79 \pm .03$$
$$\rho_{\min} \propto W^{\beta}, \quad \beta = 0.75 \pm .03$$

as demonstrated in Fig. 3 where the data have been fitted by power laws for large W. The exponent $\beta > 1$ implies that in the limit of large disorder the

DOS diverges. This is not surprising for the scaled DOS, because the scaled width of the subband shrinks. We note, however, that also in the unscaled plot the height of the peak increases with disorder W. It turns out that the approach of the peak and the minimum towards the exact centre of the subband at $E/W = \frac{1}{2}$ can also be described by power laws:

$$E(\rho_{\max})/W - 1/2 \;\propto\; W^{-\gamma}, \quad \gamma = 2.02 \pm .05$$
$$1/2 - E(\rho_{\min})/W \;\propto\; W^{-\gamma}, \quad \gamma = 1.80 \pm .04$$

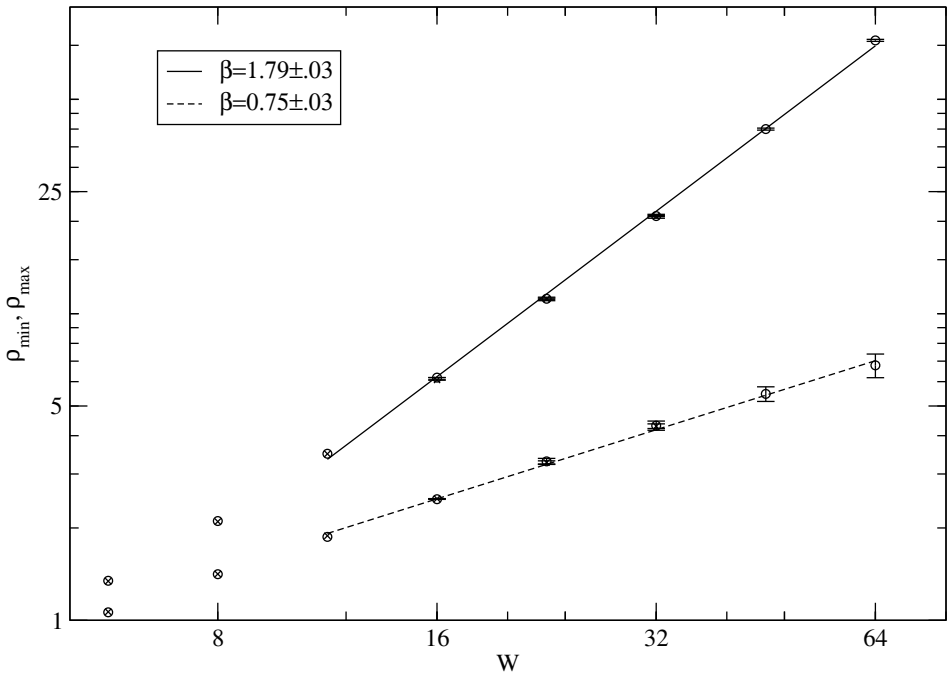

Fig. 3. Scaling of $\rho_{\min}$ and $\rho_{\max}$ with W for $L = 15$(o) and $L = 30$(x). The lines are least-squares linear fits for $L = 15$. Error bars are related to the number of missed eigenvalues.

Both exponents are close to the value 2 and might be explained by perturbation theory [28].

In summary, we have seen that the DOS of the Bernoulli–Anderson model for sufficiently strong disorder shows two separate subbands with a strong

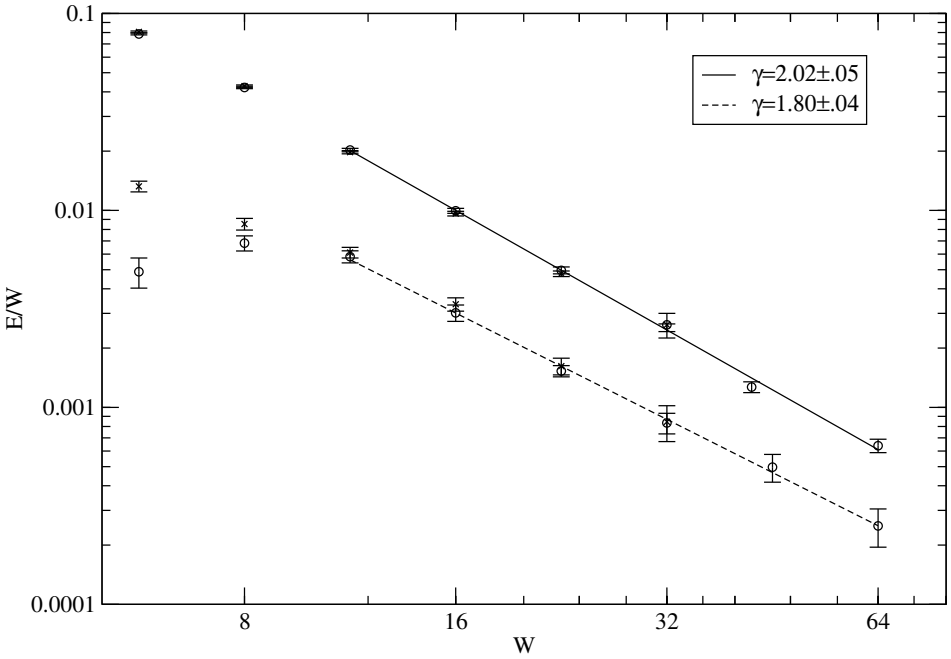

Fig. 4. Distance of the minimum (lower data) and the maximum (upper data) of the DOS from the centre of the subband. The lines are least-squares linear fits for $L = 15$. Error bars are related to the bin size of the histogram.

sharp peak near the centre in a striking contrast to the standard Anderson model with box distribution or other continuous distributions for the potential energies. A more detailed analysis of these structures will have to be performed. It is reasonable to assume that they may be connected with certain local structures of the configuration like independent dimers and trimers or other clusters separated from the rest of the system by a neighborhood of atoms of the other kind. In such a situation where all neighboring atoms belong to the other subband, the wave function at those sites would approach zero for large disorder, i.e. the space related to those sites becomes inaccessible for the electrons from the other subband. This is exactly what happens also in the quantum perculation model.

We note that there are other smaller peaks to be seen in the DOS which might be related to larger separate clusters. A more detailed analysis of these structures is under investigation. If an additional disorder is applied randomizing the potential energy as in the standard Anderson model of localization, then the peaks are quickly smeared out already for small values of this additional disorder [11].

Recently an efficient preconditioning algorithm has been proposed for the diagonalization of the Anderson Hamiltonian [29]. Previously respective shift-

and-invert techniques had been shown to be significantly faster than the standard implementation of the Lanczos algorithm, but the memory requirements where prohibitively large for moderate system sizes already, even when only a very small number of eigenvalues and eigenvectors was calculated. The new implementation reduces this problem considerably, although the memory requirement is still larger than for the standard implementation [29]. It remains an open question whether that algorithm is also superior when the calculation of the complete spectrum is required.

References

[1] P. W. Anderson. Absence of diffusion in certain random lattices. *Phys. Rev.*, 109:1492–1505, 1958.

[2] M. Aizenman, R. Sims and S. Warzel. Fluctuation based proof of the stability of ac spectra of random operators on tree graphs. ArXiv: math-ph/0510069.

[3] A. Klein. Absolutely continuous spectrum in the Anderson model on the Bethe lattice. *Math. Res. Lett. 1*, 4:399–407, 1994.

[4] F. Germinet, A. Klein, J. Schenker: announced.

[5] P. Stollmann. Caught by disorder: bound states in random media. *Progress in Mathematical Physics, Vol. 20*. Birkhäuser, Boston, 2001.

[6] M. Aizenman, A. Elgart, S. Naboko, J. Schenker, G. Stolz. Moment analysis for localization in random Schrödinger operators. ArXiv: math-ph/0308023. *Invent. Math.*, to appear.

[7] F. Wegner. Bounds on the DOS in disordered systems. *Z. Phys. B*, 44:9–15, 1981.

[8] J. Bourgain and C. Kenig. Localization for the Bernoulli–Anderson model. *Invent. Math.*, to appear.

[9] A. Alvermann and H. Fehske. Local distribution approach to the electronic structure of binary alloys. *Eur. Phys. J. B*, 48:295–303, 2005. ArXiv: cond-mat/0411516.

[10] G. Schubert, A. Weiße and H. Fehske. Localization effects in quantum percolation. *Phys. Rev. B*, 71:045126, 2005.

[11] I. V. Plyushchay, R. A. Römer and M. Schreiber. Three-dimensional Anderson model of localization with binary random potential. *Phys. Rev. B*, 68:064201, 2003.

[12] V. Janiš and J. Kolorenč. Mean-field theories for disordered electrons: Diffusion pole and Anderson localization. *Phys. Rev. B*, 71:245106, 2005. ArXiv: cond-mat/0501586.

[13] M. S. Laad and L. Craco. Cluster coherent potential approximation for electronic structure of disordered alloys. *J. Phys.: Condens. Matter*, 17:4765–4777, 2005. ArXiv: cond-mat/0409031.

[14] C. M. Soukoulis, Q. Li, and G. S. Grest. Quantum percolation in three-dimensional systems. *Phys. Rev. B*, 45:7724–7729, 1992.

[15] E. Hofstetter and M. Schreiber. Finite-size scaling and critical exponents: A new approach and its application to Anderson localization. *Europhys. Lett.*, 27:933–939, 1993.

[16] B. Simon. *Spectral analysis of rank one perturbations and applications. Mathematical quantum theory. II. Schrödinger operators (Vancouver, BC, 1993), CRM Proc. Lecture Notes Vol. 8*:109–149. Amer. Math. Soc., Providence, RI, 1995.

[17] I. Veselić. Integrated density of states and Wegner estimates for random Schrödinger operators. In C. Villegas-Blas and R. del Rio, editors, *Schrödinger operators (Universidad Nacional Autonoma de Mexico, 2001)*, volume 340 of *Contemp. Math.*, pages 98–184. Amer. Math. Soc., Providence, RI, 2004. ArXiv: math-ph/0307062.

[18] D. Hundertmark, R. Killip, S. Nakamura, P. Stollmann, I. Veselic: Bounds on the spectral shift function and the density of states. *Comm. Math. Phys.*, to appear.

[19] P. Stollmann. Wegner estimates and localization for continuum Anderson models with some singular distributions. *Arch. Math. (Basel)*, 75:307–311, 2000.

[20] J.-M. Combes, P. D. Hislop, and F. Klopp. Hölder continuity of the integrated density of states for some random operators at all energies. *Int. Math. Res. Not.*, 4:179–209, 2003.

[21] J.-M. Combes, P. D. Hislop, F. Klopp, and S. Nakamura. The Wegner estimate and the integrated density of states for some random operators. *Proc. Indian Acad. Sci. Math. Sci.*, 112:31–53, 2002. www.ias.ac.in/mathsci/.

[22] J.-M. Combes, P. D. Hislop, and S. Nakamura. The L^p-theory of the spectral shift function, the Wegner estimate, and the integrated density of states for some random Schrödinger operators. *Commun. Math. Phys.*, 70:113–130, 2001.

[23] A. Croy, R. A. Römer and M. Schreiber. Localization of electronic states in amorphous materials: recursive Green function method and the metal–insulator transition at $E \neq 0$. In K. H. Hoffmann and A. Meyer, editors, *Parallel Algorithms and Cluster Computing - Implementions, Algorithm and Applications, Lecture Notes in Computational Science and Engineering*. Springer, Berlin, 2006.

[24] B. Bulka, M. Schreiber and B. Kramer. Localization, quantum interference, and the metal–insulator transition. *Z. Phys. B*, 66:21–30, 1987.

[25] J. K. Cullum and R. A. Willoughby. *Lanczos Algorithms for Large Symmetric Eigenvalues Computations, Vol. 1, Theory*. Birkhäuser, Basel, 1985.

[26] U. Elsner, V. Mehrmann, F. Milde, R. A. Römer and M. Schreiber. The Anderson model of localization: A challenge for modern eigenvalue methods. *SIAM J. Sci. Comp.*, 20:2089–2102, 1999.

[27] M. Schreiber, F. Milde, R. A. Römer, U. Elsner and V. Mehrmann. Electronic states in the Anderson model of localization: benchmarking eigenvalue algorithms. *Comp. Phys. Comm.*, 121-122:517–523, 1999.

[28] V. Z. Cerovski. *(private communication)*.

[29] O. Schenk, M. Bollhöfer and R. A. Römer. On large scale diagonalization techniques for the Anderson model of localization. ArXiv: math.NA/0508111.